

Electronic structure of iridium silicides

M. Wittmer, P. Oelhafen,* and K. N. Tu

IBM Thomas J. Watson Research Center, Yorktown Heights, New York 10598

(Received 6 November 1985)

We present a detailed ultraviolet and x-ray photoelectron spectroscopy investigation of the electronic structure of three bulk iridium silicide compounds, IrSi, IrSi_x ($x \approx 1.6$), and IrSi₃. We observed a narrowing of the iridium *d* band and a concomitant broadening of the Si 2*p* band in the silicides which indicate that the bonding in these compounds is caused by a hybridization of the Ir *d* states and the Si *sp* hybrids. This is consistent with bonding models proposed for 3*d* and 4*d* transition-metal silicides. However, a *d*-band shift was not observed as reported in other transition-metal silicides. Also, we found that IrSi and IrSi₃ are metallic. However, we observed that IrSi_x ($x \approx 1.6$) is a semiconductor, in agreement with earlier work. We discuss this difference in terms of chemical trends in the bonding of iridium silicide compounds.

I. INTRODUCTION

Silicon and transition metals can form a variety of stable silicide compounds. Early research on silicides focused on the growth kinetics and sequence of silicide phases that form when a metal layer is reacted with silicon.¹ Later on the widespread use of silicide interfaces in semiconductor devices and the quest for the nature of the Schottky barrier have stimulated extensive studies of metal-semiconductor interfaces.² Although our knowledge of the chemical bonding and reactions at metal-semiconductor interfaces has been broadened by these studies, a unified picture of the Schottky barrier is still lacking. In comparison, much less attention has been paid to the electronic structure of bulk silicides. This knowledge is an important prerequisite for the understanding of the more complex electronic structure of silicide-silicon interfaces.

Recently, Weaver *et al.*³ have reported on a systematic study of the bonding and the band-structure properties in 3*d* transition-metal silicides from CaSi₂ through NiSi₂. They combined synchrotron radiation photoemission experiments with self-consistent augmented-spherical-wave calculations of the density of states to elucidate the dependence of the band structure on *d*-band occupancy. They found that silicon-*p*-metal-*d* mixing is important for all silicides they investigated. On the other hand, they indicated that the silicon *s* states play a relatively unimportant role in the bonding. In addition, they observed that the disilicides of Ti through Co all show an important *d* character within 3 eV of the Fermi energy (E_F) and point out that these states generally constitute the nonbonding 3*d* states. Apart from this study, photoemission results have been reported for bulk silicides of group-VIII transition metals, NiSi₂,⁴⁻⁶ Pd₂Si,⁶⁻⁸ and PtSi.⁹ The role of the metal 4*d* and 5*d* states, respectively, and silicon *s* and *p* states in the chemical bonding of Pd₂Si and PtSi are similar to the 3*d* transition-metal silicides. The *p*-*d* bonding states are found near the bottom of the *d* band at about -5.5 eV for Pd₂Si,^{7,8} and a peak of bonding states

has been observed at -4.5 eV for PtSi.⁹

In this paper we report on ultraviolet photoelectron (UPS) and x-ray photoelectron spectroscopy (XPS) studies of the electronic structure of bulk iridium silicides. These silicides are particularly interesting because they have exceptional electronic and metallurgical properties: Three stoichiometric iridium silicide compounds exist, IrSi, IrSi_x ($x \approx 1.6$), and IrSi₃. This allows the investigation of the effect of compositional changes on the electronic structure. The iridium silicides exhibit selective growth in that each silicide compound forms in a specific temperature range and only one silicide compound grows at any time.¹⁰ In addition, the barrier heights of iridium silicide Schottky diodes prepared on *n*-type silicon are the highest barrier heights known to date of any silicides.^{11,12} For this reason, it is of great interest to study the electronic properties of iridium silicide-silicon interfaces. We will report on this subject in a subsequent publication. It has been shown recently that the silicide compound IrSi_x ($x \approx 1.6$) is a semiconductor.¹³ In contrast, we will show that IrSi and IrSi₃ are metallic. This raises the intriguing question, why the silicon-poor and the silicon-rich silicides are metallic and the compound with intermediate silicon content is semiconducting. Thus, it appears that iridium silicides are interesting systems for an exploration of their electronic structure.

II. EXPERIMENTAL

The iridium silicide films used in this study were prepared in two different ways. The first set of samples was prepared by coevaporating iridium and silicon in a dual *e*-beam system on chemically cleaned Si(100) wafers. The base pressure prior to deposition of the films was 3×10^{-7} Torr. Silicide films about 1500 Å thick were then coevaporated by adjusting the individual deposition rates of iridium and silicon by means of independent crystal rate monitors to obtain a specific film composition. Subsequently the wafers were annealed in a furnace flushed with helium to complete the reaction of the iridi-

um with the silicon and to form a silicide layer of proper stoichiometry. The annealing temperatures were 400°C for IrSi, 600°C for IrSi_x ($x \approx 1.6$), and 1000°C for IrSi₃.¹⁰

The other set of samples was prepared by first evaporating iridium films of 70 and 650 Å thickness, respectively, on clean Si(100) wafers at a pressure of 5×10^{-7} Torr. The wafers with the thick iridium films were then annealed in the helium furnace at the same temperature as the coevaporated samples to form silicide layers of proper stoichiometry. Samples of the wafers with the thin iridium films were used for annealing *in situ* the ultrahigh vacuum (UHV) chamber of the photoelectron spectrometer.

For comparison purposes we have also measured the photoelectron spectra of Si(100) and polycrystalline Ir. The silicon sample was prepared from *n*-type wafers of 5 Ω cm resistivity by repeated sputtering with 1000-eV Ar⁺ ions and annealing at about 850°C for 3 min. During annealing the pressure did not rise above 2×10^{-9} Torr. This cleaning procedure produced a sharp (2×1) two-domain low-energy electron diffraction (LEED) pattern. The Fermi level was determined by subsequent evaporation of iridium onto the silicon sample.

Photoemission measurements were performed in an angle-resolved spectrometer model No. ADES 400 by Vacuum Generators, Inc. The resulting energy resolutions were 0.15 eV for UPS ($h\nu = 21.2$ eV) and 1.2 eV for XPS ($h\nu = 1253.6$ eV). The samples were loaded through an air lock into the preparation chamber. The oxide and carbon surface contaminations were removed by sputtering with 1000-eV Ar⁺ ions for 30 min, followed by a pump down of the chamber to 1×10^{-9} Torr. The samples were then annealed *in situ* to restore the proper stoichiometry and crystal structure in the surface region of the films. The annealing temperature was chosen typically 150°C higher than the corresponding annealing temperature in the helium furnace and the annealing time was 3 min. This cleaning procedure was repeated with a 10-min sputtering step and a 1-min annealing step. The samples were then ready for transfer into the analysis chamber. The cleanliness of the surface was investigated with XPS. The O 1s and C 1s core excitations were not discernible from the background noise, indicating a surface contamination of less than 1% of a monolayer of O or C.

The base pressure in the spectrometer was 2×10^{-10} Torr and rose to 1×10^{-9} Torr during the operation of the gas discharge lamp for ultraviolet photoemission. The ultraviolet photoemission spectra were obtained at 21.2 and 40.8 eV by using He I or He II radiation, respectively. For UPS, the photons were incident at 45° measured from the sample normal and the analyzer registered electrons emitted at a normal direction from the sample. The analyzer was operated in the constant-resolution mode with a pass energy of 10 eV for He I and 20 eV for He II radiation. X-ray photoemission was performed with an Mg Kα x-ray source. The angle of incidence of the x rays was 45° and the photoelectron spectra have been measured at an emission angle of 15°. The analyzer was again operated in the constant-resolution mode with a pass energy of 50 eV.

Auger electron spectroscopy (AES) measurements were

performed in the undifferentiated mode by using Mg Kα x rays as excitation source. The pass energies of the analyzer operated in the constant-resolution mode were 20 eV for the Ir *N*_{6,7} *VV* and 50 eV for the Si *L*_{2,3} *VV* transition.

In situ temperature measurements were performed with an Ircan model No. 300 infrared pyrometer. The different emittances of the iridium silicides were taken into account by comparing the temperature of a graphite spot (Aquadac) painted on the surface of a dummy sample with the temperature of the silicide film adjacent to the graphite spot. The emittance adjustment on the pyrometer was then set for equal temperature readings.

Before and after surface analysis the composition of the silicide films was analyzed with Rutherford backscattering (RBS) spectrometry. The silicide compounds were identified with glancing angle x-ray diffraction in a Seeman-Bohlin camera.

III. RESULTS AND DISCUSSION

The crystal structure of two of the thermodynamically stable iridium silicides are well known. IrSi is the silicide compound that forms first in the temperature range of 400 to 600°C (Ref. 10) in a reaction of a thin film of Ir with Si. Its crystal structure is orthorhombic and of the MnP type with lattice constants $a = 5.558$ Å, $b = 3.211$ Å, and $c = 6.273$ Å.¹⁴ The space group of IrSi is *Pnma*. The next silicide compound that forms in the temperature range of 500 to 950°C is nominally IrSi_x ($x \approx 1.6$). The stoichiometry has been reported as $x = 1.5$ (Ref. 15) to $x = 1.75$ (Ref. 10). Although the space group of this compound has not yet been determined, it is known that the crystal structure is monoclinic with $a = 5.542$ Å, $b = 14.166$ Å, $c = 12.426$ Å, and $\beta = 120.61^\circ$.^{10,13} The large unit cell presents great difficulties in the complete structure characterization of this compound. The third silicide compound, IrSi₃, forms at temperatures around 1000°C. Its crystal structure is hexagonal and of the Na₃As type with lattice constants $a = 4.350$ Å and $c = 6.630$ Å.¹⁶ The space group of IrSi₃ is *P6₃/mmc*. In view of the incomplete structural characterization of IrSi_x ($x \approx 1.6$), we start the presentation of our results with an investigation of the bulk composition of our coevaporated and reacted silicide films.

A. Bulk composition of the iridium silicide films

In Fig. 1 we present RBS spectra obtained with 2.3-MeV ⁴He⁺ particles of four different samples, the first showing the spectrum of a 650-Å-thick iridium film deposited on a silicon substrate and the others showing the spectra of the coevaporated silicide films IrSi, IrSi_x ($x \approx 1.6$), and IrSi₃ on silicon substrates. Because of the large scattering cross section of the iridium compared to the silicon, the low-energy parts of the spectra in Fig. 1, which contain the silicon profiles, have been enlarged by a factor of 5. It is clearly seen that the yield of the iridium signal decreases while that of the silicon signal increases in correspondence with the changes in stoichiometry of the films. The composition of the coevaporated silicide films can be calculated from the relative peak heights of

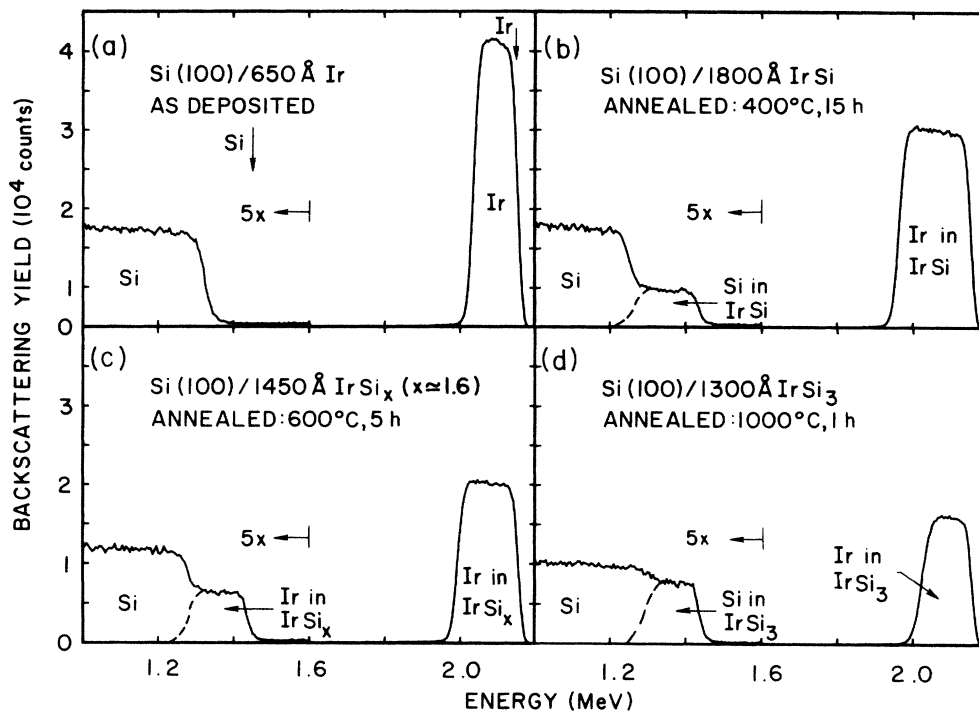


FIG. 1. 2.3-MeV $^4\text{He}^+$ RBS spectra of a polycrystalline iridium film on Si(100) and of the three iridium silicide compound films prepared by coevaporation of iridium and silicon and subsequent annealing in a helium furnace. Identical results were obtained when the polycrystalline iridium film was reacted with the silicon substrate at the temperatures indicated in the insets.

iridium and silicon.¹⁷ From the spectra of Figs. 1(b), 1(c), and 1(d), we obtain atom ratios of Si: Ir equals 1.0 ± 0.05 , 1.6 ± 0.05 , and 3.0 ± 0.05 , pointing to the compounds IrSi, IrSi_x ($x \approx 1.6$), and IrSi_3 , respectively. Because of the incomplete structure characterization of IrSi_x ($x \approx 1.6$), we refrain from assigning a chemical formula to this compound.

Positive phase identification can be obtained by x-ray diffraction. The diffraction patterns of the three coevaporated and annealed silicide films are shown in Fig. 2. The diffraction lines of IrSi and IrSi_3 have been indexed in accordance with their published powder diffraction data.^{14,16} In case of the compound IrSi_x ($x \approx 1.6$) we calculated the diffraction lines on the basis of the known lattice parameters,^{10,13} but without considering selection rules because of the unknown space group. The results of Fig. 2 confirm the compositions deduced from RBS analysis. If the samples are not annealed following coevaporation of the thin films, then x-ray diffraction reveals only a few broad lines. This indicates that mixing of iridium and silicon atoms is the main process that occurs during coevaporation, whereas the amount of silicide formation is limited. Consequently, an annealing step is required to obtain fully crystallized silicide films.

X-ray and RBS analysis do not provide information on the surface composition of the silicide films. However, this information is available with XPS core-level spectroscopy by calibrating the core-level intensities of iridium and silicon in the silicide compounds with those of the pure constituents. For that purpose we measured core-level intensities on a clean silicon sample and on one

covered with a 650-Å-thick evaporated iridium film. The agreement of surface and bulk compositions was within 10%.

B. Ultraviolet photoemission results

For each silicide compound we have investigated a number of samples which were prepared in both ways, namely by coevaporation of iridium and silicon and by reaction of an evaporated thin film of iridium with the silicon substrate. Nevertheless, we have not observed a difference in the valence-band structure of the two differently prepared sets of samples. Thus, the two methods of preparation yield identical silicide films and we will not distinguish between them in the following. However, it should be noted that we were able to form each of the three iridium silicide compounds by annealing a thin film of iridium on silicon *in situ* of the UHV chamber.

In Fig. 3 we present the valence-band spectra observed in normal emission for IrSi, IrSi_x ($x \approx 1.6$), and IrSi_3 at a photon energy of 21.2 eV. For comparison, the valence-band spectra of UHV cleaned Si(100) and of a 70-Å-thick evaporated Ir film have been included in the figure. Two features are immediately apparent in Fig. 3. The first is the broad and relative structureless appearance of the spectra for the silicides. This is due most likely to the polycrystalline microstructure of our iridium silicide films and to the large spin-orbit splitting in iridium as mentioned in the Discussion section. The second is the absence of electronic states near the Fermi energy in the valence-band spectrum of IrSi_x ($x \approx 1.6$). This points to

the existence of an energy gap of a semiconducting material. Indeed, the semiconducting nature of IrSi_x ($x \approx 1.6$) has been reported by Peterson *et al.*¹³

Band-structure calculations can be useful in interpreting the experimental emission features in photoelectron spectra. However, $5d$ transition-metal silicides necessitate the inclusion of relativistic corrections. To our knowledge such calculations have not been performed for any iridium silicide compound. In the absence of support of band-structure calculations we start our discussion of the valence-band spectra by inspecting first the spectrum of pure Ir. The electronic structure of Ir has been investigated in detail by van der Veen *et al.*¹⁸ with angle-resolved photoemission using synchrotron radiation. Their results are in reasonable agreement with recent band-structure calculations performed by Noffke and Fritsche¹⁹ and Nemoshkalenko *et al.*²⁰ These studies show that the elas-

tic spectrum (spectrum of elastically emitted electrons) is dominated by d states. As in the angle-resolved photoemission study,¹⁸ we observe two dominant peaks in the iridium spectrum shown in Fig. 3. The peak at -0.9 eV is attributed to direct transitions from the upper d band to the free-electron-like sp final-state band. van der Veen *et al.*¹⁸ observed a maximum in this transition for photon energies of $h\nu = 20.5$ eV. The other peak at -4.1 eV as well as the shoulder at -2.3 eV are due to transitions from the lower spin-orbit split d bands into the lower-energy part of the free-electron-like sp final-state band. This transition was found to be very weak at photon energies of $h\nu = 20$ – 21 eV for normal emission from both Ir(111) and Ir(100).¹⁸ However, in our case the iridium film is polycrystalline and the normal emission spectrum does not sample transitions occurring just at the Γ point but rather averages over transitions taking place in a larger part of k space. This gives rise to a larger intensity of the transition in polycrystalline samples. A texture was not observed in the microstructure of iridium films evaporated on (100) and (111) oriented silicon wafers.¹²

Other features that are observable in the valence-band spectrum of iridium are the shoulder at -1.8 eV and the structures at -8.4 and -10.9 eV. Following the interpretation of van der Veen *et al.*,¹⁸ the shoulder at -1.8 eV is attributed to transitions from the uppermost valence bands to the sp free-electron-like final-state band. The

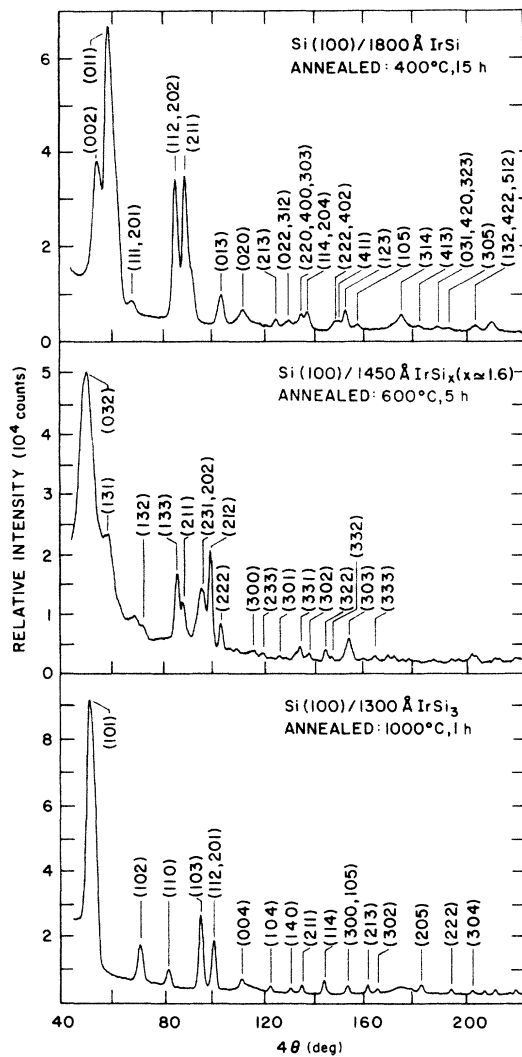


FIG. 2. X-ray diffraction patterns of the three iridium silicide compound films. The diffraction peaks of IrSi and IrSi_3 are indexed according to published powder diffraction data (Refs. 14 and 16). The indexing of the diffraction peaks of IrSi_x ($x \approx 1.6$) is based on calculated diffraction data.

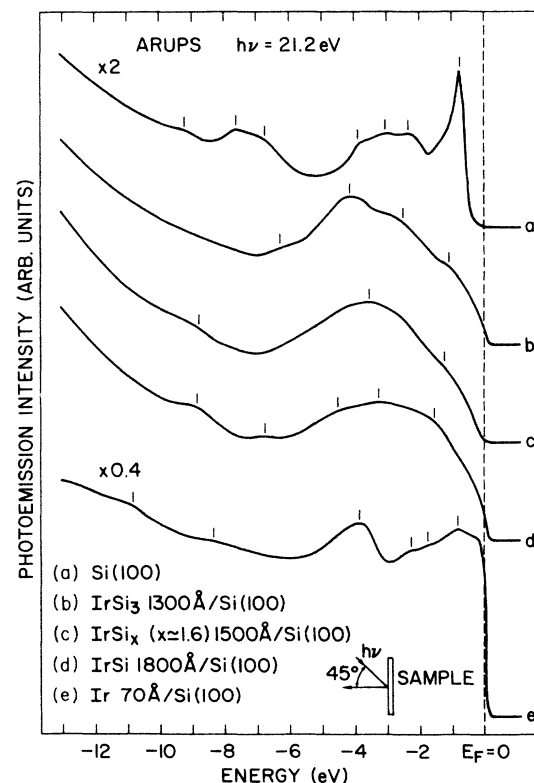


FIG. 3. Valence-band photoelectron spectra of IrSi, IrSi_x ($x \approx 1.6$), and IrSi_3 obtained in normal emission at a photon energy of $h\nu = 21.2$ eV. For comparison, the valence-band photoelectron spectra of UHV-cleaned Si(100) and of a 70-Å-thick polycrystalline Ir film are included.

structures at -8.4 and -10.9 eV may be due to a minor adsorption of carbon monoxide.²¹

Next we consider in Fig. 3 the valence-band spectrum of Si(100) obtained in normal emission. The overall shape of the spectrum is in very good agreement with published photoemission spectra of Si(100) (2×1).²² The dominant emission peak at 0.7 eV below E_F has been observed in several photoemission studies of Si(100) and originates from intrinsic surface states.²²⁻²⁴ The shoulder at -1.3 eV is also due to surface states.^{22,23} The other features of the spectrum can be associated essentially with bulk transitions. The broad emission with features at -2.4 , -3.0 , and -3.9 eV is due to emission from the p -like top valence bands.²⁵ The broad peak at -7.6 eV and the shoulder at -6.8 eV are attributed to emission from p -like states with s admixture, and the weak feature at -9.3 eV is due to the lowest s -like states.²⁵ The photoemission data of Si(100) have been interpreted reasonably well with an asymmetric dimer model.²⁶

Using the valence-band spectra of Ir and Si(100) as a reference, we can now proceed with the discussion of the valence-band structure of the iridium silicides. The valence-band spectrum of IrSi is dominated by intense emission in the region -1.0 to -5.0 eV and shows shoulders at -1.6 and -4.5 eV. This emission is due to metal d states because the large photoionization cross section of these states and the large number of valence electrons of Ir relative to Si cause the IrSi spectrum to be dominated by the Ir $5d$ band. It is apparent that the occupied state density is shifted to higher binding energies by about 0.6 eV as a result of silicide formation. The central peak of the emission intensity is at -3.3 eV and the bottom of the emission is found at -6.2 eV. The central peak shows a shift to lower energies for IrSi_{*x*} ($x \approx 1.6$) and IrSi₃. The spectrum of IrSi shows two relatively weak peaks at -6.8 and -8.9 eV. They could be attributed to Si-derived s and p states. In addition, the spectrum of IrSi has a characteristic Fermi edge which demonstrates the metallic character of IrSi.

The energy gap at E_F in the valence-band spectrum of IrSi_{*x*} ($x \approx 1.6$) distinguishes the electronic structure of this phase from the other two silicide compounds. The Fermi level is found close to the valence-band edge. A direct band gap of $E_g = 1.2 \pm 0.1$ eV was reported for IrSi_{*x*} ($x \approx 1.6$) on the basis of optical-absorption measurements.¹³ The main peak of the emission intensity in IrSi_{*x*} ($x \approx 1.6$) is at -3.6 eV with a shoulder at -1.3 eV. Finally, a feature at -8.9 eV is observable, which is seen as a peak in the spectrum of IrSi. However, the intensity of this feature in the IrSi_{*x*} ($x \approx 1.6$) spectrum is much weaker. It may also be associated with Si-derived s states.

The valence-band spectrum of IrSi₃ shows much more structure than those of IrSi and IrSi_{*x*} ($x \approx 1.6$). The emission has a marked peak at -4.2 eV and shoulders at -6.2 , -2.5 , and -1.1 eV. The existence of electronic states near E_F indicates that the silicide IrSi₃ has metallic character.

The bottom of the d band in pure iridium is found at about -5.8 eV in Fig. 3. In contrast, the iridium silicides show emission in the region of -5.5 to -7.2 eV with well-discernible features for IrSi and IrSi₃. These emis-

sion features can be associated with bonding orbitals and are likely to stem from states which have been pulled down from the d band by the bonding between iridium and silicon.

It is informative to complement UPS spectra obtained with He I radiation with spectra taken with He II radiation. At higher photon energies the photoelectron spectra represent more closely the density of the initial states because the influence of the final states in the photoionization process is reduced. Also, emission from states with d character is emphasized. In Fig. 4 we show UPS spectra of pure iridium and the three silicides at a photon energy $h\nu = 40.8$ eV. The relative intensity of the d -band emissions are now much stronger as a result of the higher photon energy. It is clearly seen that the widths of the d bands are very similar for the three silicides, but significantly smaller than that of pure iridium. The bottom of the d band is at about -8.5 eV for pure iridium and at about -6.5 eV for its silicides. The d bands have a common emission peak at -3.7 eV. This is in contrast to the trend of the main emission peak observed at a photon energy $h\nu = 21.2$ eV which shifts towards higher binding energy with increasing silicon atoms per unit formula. We believe that this discrepancy arises mainly from a difference in photoelectron excitation cross sections across the emission band.²⁷ Lower photon energies emphasize the electron states near E_F .^{28,29} For IrSi, which has a high density of states near E_F , the maximum of the emission appears thus closer to E_F . In contrast, IrSi₃ has a lower density of states near E_F , and hence the maximum of the

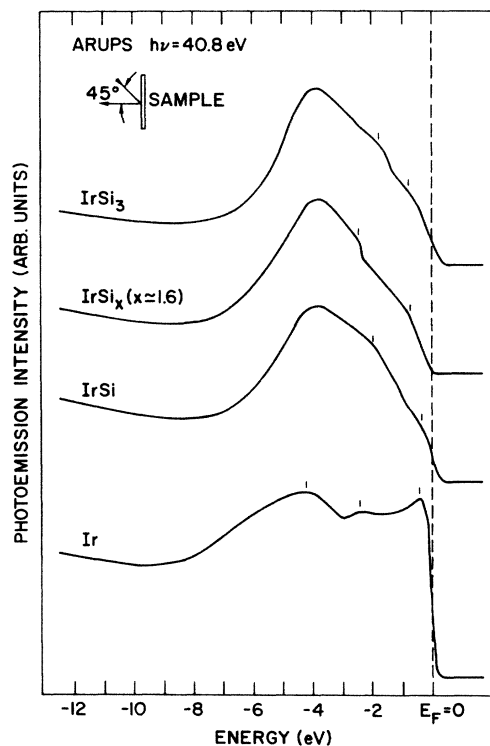


FIG. 4. Valence-band photoelectron spectra of IrSi, IrSi_{*x*} ($x \approx 1.6$), and IrSi₃ obtained in normal emission at a photon energy of $h\nu = 40.8$ eV. Note the absence of a shift of the d -band maximum.

emission turns up at lower energy. Higher photon energies do not emphasize the electron states near E_F and, consequently, a shift of the emission peak is not observed. Thus we conclude from Fig. 4 that the d bands become much narrower in the silicides but that a clear shift of the d bands is not observed. With He I radiation amplitude is picked up from d states with p and s admixture and results in the emission features observed at the low-energy side of the d band. These features which are attributed to bonding orbitals are not discernible at a photon energy $h\nu=40.8$ eV because they do not have pure d character and because the signal-to-noise ratio with He II excitation is much inferior to that with He I excitation. Nevertheless, several additional features can be found in the spectra of Fig. 4. There are shoulders at -0.4 and -2.0 eV for IrSi, -0.7 and -2.4 eV for IrSi $_x$ ($x \approx 1.6$), and -0.6 and -1.6 eV for IrSi $_3$. Finally, the spectrum of IrSi $_x$ ($x \approx 1.6$) exhibits a gap at E_F , in accordance with the result of Fig. 3.

C. x-ray photoemission results

The core-level transitions of iridium and silicon have been investigated with x-ray photoemission in order to obtain information on the nature of the chemical bonding in iridium silicides. In Table I we present the results of an investigation of the Ir $4f$ and Si $2p$ core-level transitions for the three iridium silicide compounds and their constituents. Table I shows the binding energy, E_B , and the asymmetry parameter, a/b , of the $4f_{7/2}$ transition. The asymmetry of the core-level line has been determined in the following way. The line shows a broadening for higher binding energies. The shape of the line can be approximated by two Gaussian distributions with different variances. The quotient of the two variances was used to quantify the asymmetry of the line. Thus, an asymmetry parameter of 1.0 corresponds to a perfectly symmetric line shape.

A comparison of the binding energy of the Ir $4f_{7/2}$ core level in pure iridium and the iridium silicides indicates that the binding energy is shifted for the silicide compounds. This chemical shift, ΔE_B , is different for the three silicide compounds. IrSi shows a very small chemical shift of 0.10 eV towards lower binding energies. This number is an average of a systematic chemical shift observed on six different IrSi samples. In contrast, the silicide compounds IrSi $_x$ ($x \approx 1.6$) and IrSi $_3$ show a chemical shift of this core level of 0.50 and 0.55 eV, respectively, to higher binding energies. A chemical trend is also notice-

able in the asymmetry parameter of the Ir $4f_{7/2}$ core line. The asymmetry of the line is high for pure Ir.³⁰ For IrSi it is intermediate and drops to a value near 1.0 for IrSi $_x$ ($x \approx 1.6$) and IrSi $_3$, indicating that the line shape becomes more symmetric with increasing silicon atoms per formula unit. The asymmetry in core-level lines can be interpreted as originating from satellite lines.³¹ Satellite lines usually occur if the photoionization process causes the transition of an electron from a filled valence-band state across the Fermi level into an empty conduction-band state. Since there are numerous states involved in this many-electron process, a tail on the high-binding-energy side of the core line is observed rather than discrete satellite lines. This tail represents a continuous distribution of satellite lines and is due to electron-hole excitations near E_F . A decrease in the local density of states leads to a decrease in the probability for the excitation of electrons at E_F and in turn to a decrease in the core-level asymmetry.³⁰ The reduced asymmetry of the Ir $4f_{7/2}$ core line in the silicide compounds is thus consistent with the low Fermi-level state densities resulting from the narrowing of the d bands. This d -band narrowing and the concomitant chemical shifts are clear fingerprints of the nature of the chemical bonding in the iridium silicide compounds.

Chemical shifts are also found for the Si $2p$ core-level lines. For the metallic silicide compounds IrSi and IrSi $_3$ the shifts are 0.30 and 0.20 eV, respectively, towards higher binding energy. In contrast to these metallic silicides, a marked shift of 0.60 eV towards higher binding energy is found for the semiconducting silicide compound IrSi $_x$ ($x \approx 1.6$). We could not resolve the spin-orbit split Si $2p$ doublet in our spectra because the separation of the $2p_{1/2}$ and $2p_{3/2}$ peaks amounts only to 0.61 ± 0.01 eV,³² which is below the resolution limit of our instrument in the XPS mode. For that reason we do not discuss the asymmetry of the Si $2p$ core line. However, the binding energy of the Si $2p$ core level listed in Table I is in excellent agreement with the mean of the published binding energies of the doublet ($2p_{1/2}$: 99.2 eV; $2p_{3/2}$: 99.8 eV).³³

D. Auger electron spectroscopy results

In general, it is very difficult to extract information on the electronic structure of concentrated alloys and compounds from Auger electron spectroscopy alone, because three electrons are involved in the excitation process. Of particular interest in the present study is the structure of the valence band. For that purpose it is important to investigate the Auger transitions which involve valence elec-

TABLE I. Binding energy, chemical shifts, and asymmetry parameter of core-level excitations in iridium silicides and their constituents. E_B calibration: $E_B^{\text{Au } 4f_{7/2}} = 84.0$ eV.

Material	Ir $4f_{7/2}$			Si $2p$	
	E_B (eV)	ΔE_B (eV)	a/b	E_B (eV)	ΔE_B (eV)
Ir	60.80 \pm 0.05		1.35		
IrSi	60.70 \pm 0.05	-0.10	1.25	99.80 \pm 0.05	+ 0.30
IrSi $_x$ ($x \approx 1.6$)	61.30 \pm 0.05	+ 0.50	1.10	100.10 \pm 0.05	+ 0.60
IrSi $_3$	61.35 \pm 0.05	+ 0.55	1.15	99.70 \pm 0.05	+ 0.20
Si				99.50 \pm 0.05	

tron states. Such investigations are only meaningful for bandlike transitions. A transition is bandlike if the relative magnitude of the bandwidth W is larger than the effective Coulomb interaction U_{eff} . If $W < U_{\text{eff}}$, then the transition is atomiclike and information on the valence-band structure is obscured by large Coulomb interactions of the two final holes.³¹ In the present case, the transitions are bandlike and in combination with XPS useful information can be obtained, particularly if the same electron states are investigated with both methods. For this reason we have performed AES analysis of the iridium silicides in the undifferentiated mode by using Mg $K\alpha$ x rays as the excitation source.

In Fig. 5 we present Si $L_{2,3}VV$ Auger spectra of UHV-cleaned Si(2×1) and of the three iridium silicides. Two features are immediately apparent in Fig. 5: The Auger spectra of the silicides show considerable line broadening compared to the spectrum of pure silicon, and a chemical shift of the Auger peak for the silicides is not discernible for IrSi and IrSi₃. The broadening of the Si $L_{2,3}VV$ line is an indication of the involvement of the valence electrons of Si in the bonding orbitals. A close inspection of the Si $L_{2,3}VV$ Auger peak position for IrSi_x ($x\approx 1.6$) reveals a small shift of 0.3 eV to lower energies. The implications of this shift on the electronic structure of IrSi_x

($x\approx 1.6$) will be discussed in the next section.

Spectra of the Ir $N_{6,7}VV$ Auger transition are shown in Fig. 6 for an evaporated Ir film and for the three iridium silicides. In contrast to the Si $L_{2,3}VV$ Auger transitions, the $N_{6,7}VV$ transitions of Ir exhibit a marked chemical shift towards lower energies and a narrowing for the three silicides. The chemical shifts observed in Fig. 6 amount to -2.6, -3.3, and -2.7 eV for IrSi, IrSi_x ($x\approx 1.6$), and IrSi₃, respectively. These shifts are significantly larger than the photoelectron $4f_{7/2}$ chemical shifts listed in Table I. This fact is in agreement with general observations of Auger and photoelectron chemical shifts.

E. Discussion

We start the discussion by commenting on the valence-band structure of the iridium silicides. The UPS spectra presented above demonstrate clearly that both IrSi and IrSi₃ are metallic, but that IrSi_x ($x\approx 1.6$) is a semiconductor. The metallic nature of IrSi and IrSi₃ is not surprising since the majority of transition-metal silicides possesses metallic character. It is one of the properties that is responsible for the widespread use of silicides in silicon semiconductor devices. On the other hand, the semiconducting nature of IrSi_x ($x\approx 1.6$) is unexpected. Only a few transition-metal silicides are known to be a

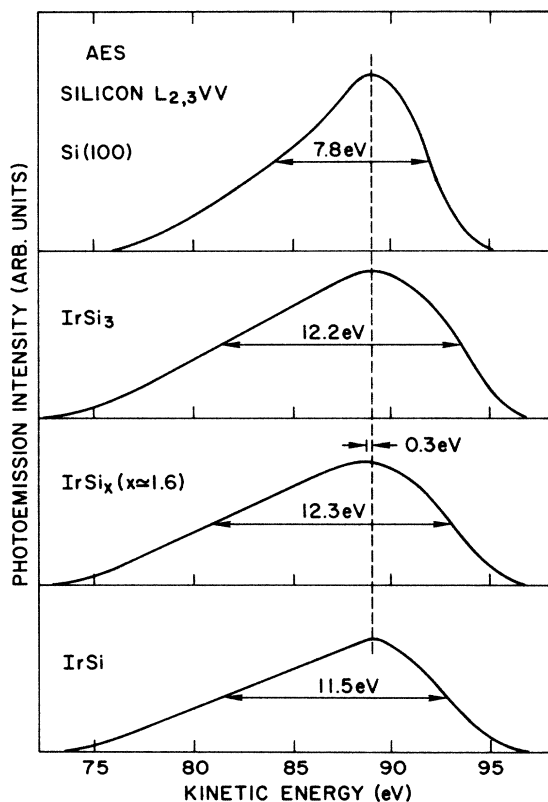


FIG. 5. Silicon $L_{2,3}VV$ Auger spectra observed with Mg $K\alpha$ excitation in the undifferentiated mode from UHV-cleaned Si(100) and the iridium silicide compounds IrSi, IrSi_x ($x\approx 1.6$), and IrSi₃. Except for a small chemical shift in case of IrSi_x ($x\approx 1.6$) the Auger peaks of IrSi and IrSi₃ show no shift but considerable broadening.

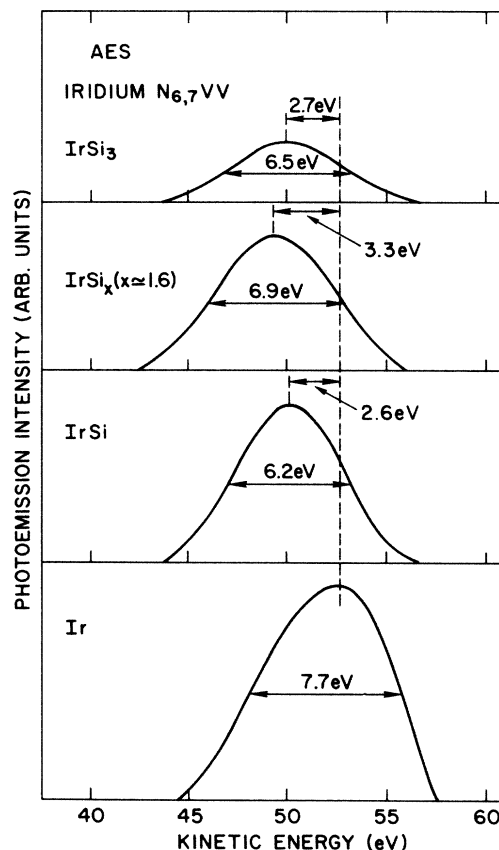


FIG. 6. Iridium $N_{6,7}VV$ Auger spectra observed with Mg $K\alpha$ excitation in the undifferentiated mode from polycrystalline iridium and the iridium silicide compounds IrSi, IrSi_x ($x\approx 1.6$), and IrSi₃. Note the chemical shift of the Auger peaks for the silicides.

semiconductor, the most prominent ones being CrSi_2 ,³⁴ Mg_2Si ,³⁵ and MnSi_2 .³⁶ Often, semiconducting silicides are highly doped and show good electrical conductivity. This is due to minor departures from the exact stoichiometry as given by the chemical formula. In the case of IrSi_x ($x \approx 1.6$) the Fermi level was found close to the top of the valence band, which is characteristic of a *p*-type semiconductor. Indeed, a preliminary investigation by Petersson *et al.*¹³ revealed that IrSi_x ($x \approx 1.6$) is a hole conductor. The semiconducting nature of IrSi_x ($x \approx 1.6$) is also manifested in studies on the thermal oxidation of silicide thin films.³⁷ The linear term of the formation kinetics of SiO_2 on IrSi_x ($x \approx 1.6$) was found to be much smaller than that for metallic silicides and comparable to that of pure silicon. It was proposed that the lower density of states at the Fermi level impedes charge transfer between the oxygen atoms and the oxidizing material, thus slowing the oxidation of thin films of IrSi_x ($x \approx 1.6$).

The absence of a *d*-band shift in the iridium silicides to higher binding energies is in contrast to *d*-band shifts observed in other transition-metal silicides such as Pt silicides,⁹ Pd_2Si ,^{6,7} and Ni silicides.⁶ Rather, we observed a narrowing of the *d* band in the iridium silicides. In particular, the density of states associated with the upper spin-orbit split *d* band in pure iridium is much attenuated in its silicides. It is likely that these states are pulled down to higher binding energies in the silicides. Only a weak feature at -0.9 eV in the iridium-rich silicide IrSi can be attributed to these states. Also, emission from the lower spin-orbit split *d* band is much reduced in the silicides compared to pure iridium. This is clearly seen at the higher photon energy. However, at the lower photon energy we observed new emission features which we associated with bonding orbitals. These findings are a clear indication that the valence *d* electrons of the transition metals participate in the chemical bonding between metal and silicon atoms. The bond is formed by a hybridization of the *d* states of the transition metal with the valence states of the silicon which creates a bonding hybrid that is more tightly bound than either of the states from which it is formed.³⁸ These bonding hybrids can be identified with the structures observed at energies between -5.5 and -7.2 eV in Fig. 3. Some of the *d* states do not participate in the bonding and constitute the nonbonding states. They can be associated with the emission peak around -4 eV in Figs. 3 and 4. We have also found that the width of the *d* band is much smaller in the silicides than in pure iridium. This is expected because the insertion of silicon atoms into the transition-metal lattice to form silicide compounds pulls the transition metals farther apart, resulting in a decrease of the width of the *d* band.³⁹ The bonding model implies that the Si *s* states are relatively unimportant in the bonding of iridium silicides. Indeed, we found that the Si *s*-derived states in IrSi and IrSi_x ($x \approx 1.6$) are unchanged at -8.9 eV. Finally, we would like to stress that we observed the same iridium silicide compounds at the surface of the samples as in the bulk of the thin films.

Next we turn to the discussion of the core level and Auger data. Table I shows that the asymmetry of the Ir $4f_{7/2}$ core-level line is significantly smaller for the silicide

compounds than for the pure metal. This is in agreement with our finding that the local Ir *5d* density of states at E_F decreases in the silicides due to a narrowing of the *d* band. The compound IrSi_x ($x \approx 1.6$) has the least asymmetry of the Ir $4f_{7/2}$ core-level line because it has the least density of states at E_F due to the existence of a gap. The trend in the asymmetry of the Ir $4f_{7/2}$ core-level line is also in accordance with the shift of the Ir $N_{6,7}VV$ Auger transition. IrSi_x ($x \approx 1.6$) has the largest Auger shift (Fig. 6), indicating that the top of its valence band is shifted most to lower energies.

The broadening of the Si $L_{2,3}VV$ Auger spectra of the silicides indicates that the occupied Si *sp* band is broader in the silicide than in pure silicon. Band-structure calculations⁴⁰ have shown that in metal-rich silicides such as Ni_3Si the Si *s* and *p* orbitals dehybridize, whereas in silicon-rich silicides such as NiSi_2 and CoSi_2 the sp^3 hybridization in the Si atoms is preserved. From this point of view the bonding in silicon-rich silicides has similarities with that in bulk silicon. Thus, the broadening of the Si $L_{2,3}VV$ Auger peak in the silicon-rich iridium silicides IrSi_x ($x \approx 1.6$) and IrSi_3 infers that the Si sp^3 hybrids participate in the chemical bonding between transition metal and silicon, whereas in IrSi only the Si *p* states do. The interaction between Si sp^3 hybrids and the Ir *5d* states appears to be strong and constitutes the bonding in the iridium silicides.

We have mentioned that the Si $L_{2,3}VV$ Auger peak of IrSi_x ($x \approx 1.6$) is shifted to lower energies by about 0.3 eV. This shift is consistent with a larger Si $2p$ binding-energy shift by the same amount as compared to the metallic iridium silicides. It is also manifested by a valence-band shift of a similar amount as observed with UPS in Fig. 3. On the other hand, the Ir $N_{6,7}VV$ Auger transition exhibits large shifts. The reason is that the Ir *4f* core levels shift only a little whereas the valence bands shift considerably and contribute twice to the Auger shift.

The energy of an Auger transition is dominated by the binding energy of the initially ionized core levels. Terms of lesser importance in a bandlike Auger transition are the Coulomb energy of the two holes and the two-hole final-state relaxation energy. In general, the binding energy of the initial state as well as the relaxation energy change when the chemical environment changes. Assuming that the Coulomb energy is the same in Ir and its silicides, we can determine the difference in Auger chemical shift $\Delta E(jkl)$ and photoelectron chemical shift ΔE_B according to

$$\Delta E(jkl) - \Delta E_B = 2\Delta R(kl) = \Delta\alpha.$$

This difference $\Delta\alpha$, where α is known as the Auger parameter,⁴¹ is then due to differences in the final-state relaxation energies $\Delta R(kl)$ between chemical states. We have listed the results of this calculation in Table II. It can be observed from Table II that the largest difference for the Ir as well as the Si transition occurs for the silicide IrSi_x ($x \approx 1.6$). Conductive materials have a higher Auger parameter than insulating compounds.⁴¹ Thus a smaller difference in the Auger parameter is expected between Ir and its metallic silicides. Table II demonstrates

TABLE II. Auger shifts, core-level shifts, and Auger parameter differences for the iridium silicide compounds in eV.

Material	Ir			Si		
	$\Delta E(NVV)$	$\Delta E_B(4f)$	$\Delta\alpha$	$\Delta E(LVV)$	$\Delta E_B(2p)$	$\Delta\alpha$
IrSi	-2.6	-0.10	-2.5	0	0.30	-0.3
IrSi _x ($x \simeq 1.6$)	-3.3	0.50	-3.8	-0.3	0.60	-0.90
IrSi ₃	-2.7	0.55	-3.3	0	0.20	-0.2

that this is the case.

So far, our discussion has presented a consistent picture of the electronic structure of the three iridium silicide compounds under study, but has not yet delivered any explanation as to why one of the silicides is semiconducting while the other two are metallic. Therefore, in the remainder of our discussion we will try to shed some light on this issue. The answer to this interesting question is related to the bonding mechanism in transition-metal silicides. Our results show enough evidence that bonding in iridium silicides is established through hybridization of Ir $5d$ and Si sp states. This type of bonding has been proposed for all transition-metal silicides investigated to date and is characteristic for compounds formed between transition metals and elements with only s and p electrons in their valence shells.³⁹

The spin-orbit splitting in pure iridium is about 1 eV.^{18,19} This large splitting leads to a broad d -band structure in the iridium silicides which is partly responsible for the broad and featureless photoemission spectra.

The hybridization of the transition-metal d states with the silicon sp states creates bonding as well as antibonding states. The formation of bonding and antibonding states opens a quasigap in the density of states near E_F . In metal-rich silicides the bonding states are generally occupied with electrons and the antibonding states are empty. This places the Fermi energy in the middle of the quasigap as is confirmed from band-structure calculations of Pd₃Si,⁷ Ni₃Si,⁴² and V₃Si.⁴³ However, the quasigap never develops into a real gap. There are always states near E_F because the band of nonbonding states is broad due to strong metal-metal interactions and overlaps E_F . For silicon-rich silicides, such as IrSi₃, the silicon-silicon interactions dominate and lead to a large density of states at E_F . This causes the quasigap to disappear. The band structure of these silicides has much in common with metallic silicon. This explains the metallic nature of IrSi₃.

Between these two extremes of composition are the silicides IrSi and IrSi_x ($x \simeq 1.6$). A small compositional difference is responsible for a change from metallic to semiconducting behavior. The semiconducting behavior necessitates that the quasigap develops into a real gap. This can happen under the following circumstances. Metal-metal and silicon-silicon interactions need to be minimized, leading to strong covalent bonding between metal and silicon atoms. The band of nonbonding states near E_F needs to be narrowed by increasing interatomic distances between metal atoms. If both conditions are ful-

filled, then a real gap may develop between nonbonding and antibonding states. Intuitively one expects this to occur for an intermediate composition of perhaps 50% metal and 50% silicon. However, we found IrSi to be metallic. Thus, it is likely that a small density of nonbonding states at the Fermi level is responsible for the metallic nature of IrSi. On the other hand, IrSi_x ($x \simeq 1.6$), which has a slightly richer silicon content, apparently has the proper stoichiometry that puts the Fermi level into the gap. This makes it a semiconductor. Presently, the details of the electronic levels in IrSi_x ($x \simeq 1.6$) cannot be worked out because its structure is not yet fully characterized. If the silicon content per unit formula is further increased, then antibonding states are being filled and the quasigap is shifted to below E_F . This has been observed in band-structure calculations of VSi₂ (Ref. 43) and WSi₂ (Ref. 44) and the $3d$ transition-metal disilicides.^{3,40} The small but finite density of states at E_F is due to contributions from antibonding states as well as from silicon-silicon interactions, and accounts for the metallic character of these silicides.

Finally, it is interesting to note that negligible Fermi-level state densities are representative of systems with energetically favorable atomic arrangements.⁴⁵ This accounts for the remarkable thermal stability of IrSi_x ($x \simeq 1.6$) in the temperature range of 500 to 950°C.¹⁰ Arguments similar to the above may be advanced for Ru₂Si₃, which apparently is another semiconducting silicide.³⁷

IV. CONCLUSIONS

Our UPS and XPS measurements have shown that IrSi and IrSi₃ are metallic whereas IrSi_x ($x \simeq 1.6$) is semiconducting. The semiconducting nature of IrSi_x ($x \simeq 1.6$) is consistent with published results on optical absorption in this silicide compound. In contrast to other transition-metal silicides, we did not observe a d -band shift in the iridium silicides. Rather, we found a narrowing of the d band and a concomitant broadening of the Si $2p$ band in the silicides, indicating that a hybridization of Ir d states and Si sp hybrids constitute the bonding in these compounds. The information we obtained from the different experimental data yields a consistent picture of the chemical bonding and the electronic structure in these silicides. We propose a model which explains the semiconducting nature of IrSi_x ($x \simeq 1.6$). Band-structure calculations would be helpful in substantiating this model.

ACKNOWLEDGMENTS

We thank the Center for Scientific Services (CSS) at Yorktown for the preparation of the samples. It is our pleasure to acknowledge invaluable discussions with J. L.

Freeouf, J. D. Tersoff, V. L. Moruzzi, and A. R. Williams. We are also grateful to S. T. Pantelides for a careful review of the manuscript. One of us (P.O.) would like to thank the Yorktown Research Lab for making his stay there possible during the course of the work.

- *Permanent address: Department of Physics, University of Basel, Klingelbergstrasse 82, 4056 Basel, Switzerland.
- ¹K. N. Tu and J. W. Mayer, in *Thin Films—Interdiffusion and Reactions*, edited by J. M. Poate, K. N. Tu, and J. W. Mayer (Wiley, New York, 1978), p. 359.
- ²See reviews by L. J. Brillson, *J. Phys. Chem. Solids* **44**, 703 (1983); and M. Schlüter, *Thin Solid Films* **93**, 3 (1982).
- ³J. H. Weaver, A. Franciosi, and V. L. Moruzzi, *Phys. Rev. B* **29**, 3293 (1984).
- ⁴Y.-J. Chang and J. L. Erskine, *Phys. Rev. B* **26**, 7031 (1982).
- ⁵Y. J. Chabal, D. R. Haman, J. E. Rowe, and M. Schlüter, *Phys. Rev. B* **25**, 7598 (1982).
- ⁶P. J. Grunthaner, F. J. Grunthaner, A. Madhukar, and J. W. Mayer, *J. Vac. Sci. Technol.* **19**, 649 (1981).
- ⁷P. S. Ho, G. W. Rubloff, J. E. Lewis, V. L. Moruzzi, and A. R. Williams, *Phys. Rev. B* **22**, 4784 (1980).
- ⁸A. Franciosi and J. H. Weaver, *Phys. Rev. B* **27**, 3554 (1983).
- ⁹P. J. Grunthaner, F. J. Grunthaner, and A. Madhukar, *J. Vac. Sci. Technol.* **20**, 680 (1982).
- ¹⁰S. Peterson, J. Baglin, W. Hammer, F. d'Heurle, T. S. Kuan, I. Ohdomari, J. de Sousa Pires, and P. Tove, *J. Appl. Phys.* **50**, 3357 (1979).
- ¹¹I. Ohdomari, K. N. Tu, F. M. d'Heurle, T. S. Kuan, and S. Peterson, *Appl. Phys. Lett.* **33**, 1028 (1978).
- ¹²I. Ohdomari, T. S. Kuan, and K. N. Tu, *J. Appl. Phys.* **50**, 7020 (1979).
- ¹³S. Peterson, J. A. Reimer, M. H. Brodsky, D. R. Campell, F. d'Heurle, B. Karlsson, and P. A. Tove, *J. Appl. Phys.* **53**, 3342 (1982).
- ¹⁴Powder Diffraction File No. 10-206, Joint Committee on Powder Diffraction Standards (International Center for Diffraction Data, Swarthmore, 1984).
- ¹⁵I. Engström and F. Zackrisson, *Acta Chem. Scand.* **24**, 2109 (1970).
- ¹⁶Powder Diffraction File No. 19-598, Joint Committee on Powder Diffraction Standards (International Center for Diffraction Data, Swarthmore, 1984).
- ¹⁷W.-K. Chu, J. W. Mayer, and M.-A. Nicolet, *Backscattering Spectrometry* (Academic, New York, 1978), p. 105.
- ¹⁸J. F. van der Veen, F. J. Himpsel, and D. E. Eastman, *Phys. Rev. B* **22**, 4226 (1980).
- ¹⁹J. Noffke and L. Fritsche, *J. Phys. F* **12**, 921 (1982).
- ²⁰V. V. Nemoshkalenko, V. N. Antonov, and V. N. Antonov, *Phys. Status Solidi B* **99**, 471 (1980).
- ²¹T. N. Rhodin, J. Kanski, and C. Brucker, *Solid State Comm.* **23**, 723 (1977).
- ²²F. J. Himpsel and D. E. Eastman, *J. Vac. Sci. Technol.* **16**, 1297 (1979).
- ²³R. I. G. Uhrberg, G. V. Hansson, J. M. Nicholls, and S. A. Flodström, *Phys. Rev. B* **24**, 4684 (1981).
- ²⁴J. E. Rowe and H. Ibach, *Phys. Rev. Lett.* **32**, 421 (1974).
- ²⁵L. Ley, M. Cardona, and R. A. Pollak, in *Photoemission in Solids II*, Vol. 27 of *Topics in Applied Physics*, edited by L. Ley and M. Cardona (Springer, New York, 1979), p. 15.
- ²⁶D. J. Chadi, *Phys. Rev. Lett.* **43**, 43 (1979); J. Ihm, M. L. Cohen, and D. J. Chadi, *Phys. Rev. B* **21**, 4592 (1980).
- ²⁷A. DasGupta, P. Oelhafen, U. Gubler, R. Lapka, H.-J. Güntherodt, V. L. Moruzzi, and A. R. Williams, *Phys. Rev. B* **25**, 2160 (1982); S. Hüfner, G. K. Wertheim, and J. H. Wernick, *Solid State Comm.* **17**, 417 (1975).
- ²⁸S. T. Manson and J. W. Cooper, *Phys. Rev.* **165**, 126 (1968).
- ²⁹H. Höchst, S. Hüfner, and A. Goldman, *Phys. Lett.* **57A**, 265 (1976).
- ³⁰G. K. Wertheim and L. R. Walker, *J. Phys. F* **6**, 2297 (1976).
- ³¹J. C. Fuggle, in *Electron Spectroscopy: Theory, Techniques and Applications*, edited by C. R. Brundle and A. D. Baker (Academic, New York, 1981), Vol. 4, p. 111.
- ³²F. J. Himpsel, P. Heimann, T.-C. Chiang, and D. E. Eastman, *Phys. Rev. Lett.* **45**, 1112 (1980).
- ³³Appendix in *Photoemission in Solids I*, Vol. 26 of *Topics in Applied Physics*, edited by L. Ley and M. Cardona (Springer, New York, 1978), p. 265.
- ³⁴I. Nishida and T. Sakata, *J. Phys. Chem. Solids* **39**, 499 (1978); D. Shinoda, S. Asanabe, and Y. Sasaki, *J. Phys. Soc. Jpn.* **19**, 269 (1964).
- ³⁵R. G. Morris, R. D. Reddin, and G. C. Danielson, *Phys. Rev.* **109**, 1909 (1958).
- ³⁶I. Nishida, *J. Mater. Sci.* **7**, 435 (1972).
- ³⁷J. E. E. Baglin, F. M. d'Heurle, and C. S. Petersson, *J. Appl. Phys.* **54**, 1849 (1983); F. M. d'Heurle, R. D. Frampton, E. A. Irene, H. Jiang, and C. S. Petersson, (unpublished).
- ³⁸O. Bisi and C. Calandra, *J. Phys. C* **14**, 5479 (1981).
- ³⁹C. D. Gelatt, Jr., A. R. Williams, and V. L. Moruzzi, *Phys. Rev. B* **27**, 2005 (1983).
- ⁴⁰J. Tersoff and D. R. Hamann, *Phys. Rev. B* **28**, 1168 (1983).
- ⁴¹C. D. Wagner, *Farad. Discuss. Chem. Soc.* **60**, 291 (1975); D. Briggs and M. P. Seah, *Practical Surface Analysis* (Wiley, New York, 1983), p. 124.
- ⁴²D. M. Bylander, L. Kleinman, and K. Mednick, *Phys. Rev. B* **25**, 1090 (1982).
- ⁴³O. Bisi and L. W. Chiao, *Phys. Rev. B* **25**, 4943 (1982).
- ⁴⁴B. K. Bhattacharyya, D. M. Bylander, and L. Kleinman, *Phys. Rev. B* **31**, 2049 (1985).
- ⁴⁵V. L. Moruzzi, P. Oelhafen, and A. R. Williams, *Phys. Rev. B* **27**, 7194 (1983).